NJC

PAPER

View Article Online
View Journal

Cite this: DOI: 10.1039/c7nj01406f

Acyclonucleosides bearing coplanar arylethynyltriazole nucleobases: synthesis, structural analysis, and biological evaluation†

Mimi Chen,[a] Zhengwei Zhou,[a] Yaxiong Suo,[a] Mengyao Li,[a] Jianhua Yao,[b] Ling Peng[c] and Yi Xia*[a]

Received 27th April 2017,
Accepted 4th July 2017

DOI: 10.1039/c7nj01406f

rsc.li/njc

Nucleoside derivatives are an important class of molecules in the search for bioactive compounds. In our continuing efforts to develop novel nucleoside analogs, we used the Sonogashira cross-coupling reaction to synthesize 1,2,4-triazole acyclonucleosides bearing various arylethynyl groups on the triazole nucleobase. By employing 3-iodotriazole nucleoside as the coupling substrate, the Sonogashira reaction proceeded efficiently even with alkynes, which are notoriously unreactive and challenging. Further crystal structural analysis unveiled the coplanar feature of the 3-arylethynyltriazole motifs, suggesting their potential as surrogates for large planar aromatic systems or nucleobases. Most importantly, several synthesized compounds displayed interesting antiproliferative activity against various cancer cells and induced apoptosis, highlighting that this family of triazole nucleosides might show promise as anticancer candidates.

Introduction

Nucleoside analogs are structurally characterized by the conjugation of various nucleobases and sugar moieties *via* a glycosidic bond.[1] Many of them can be considered as synthetic mimics of natural nucleosides in terms of their metabolism and ability to be incorporated into DNA and/or RNA, which leads to the inhibition of nucleic acid synthesis and consequent antimetabolite activity.[2,3] Nowadays, nucleoside analogs form an important family of bioactive compounds in drug discovery thanks to their pharmacologically diverse applications as antiviral, anticancer, antimicrobial, and immunomodulatory agents.[4,5]

Among the various nucleoside mimics, besides the nucleosides with modifications of the ribose sugar component,[6–9] those carrying unusually modified nucleobases have attracted considerable attention. This is because using nonnatural heterocycles as nucleobases improves the *in vivo* stability and also imparts new biologically interesting activities involving novel modes of action.[10–13] For example, ribavirin, a synthetic nucleoside bearing the nonnatural heterocycle 1,2,4-triazole as the nucleobase (Fig. 1), exhibits broad-spectrum antiviral activity against a variety of different viruses.[14,15] It has served as a candidate drug to treat a panel of emerging viruses for more than 40 years and is still clinically important in the treatment of hepatitis C virus (HCV) today.[16–18] Recently, ribavirin has also been reported to exhibit anticancer activity, and has been tested in clinical trials against acute myeloid leukemia.[19–21]

The unique and interesting therapeutic potency of ribavirin motivated us to develop 1,2,4-triazole nucleoside analogs in the quest for new structural paradigms to combat global viral infection and cancer malignancy.[22] Consequently, myriad 1,2,4-triazole nucleosides with modifications made on the triazole nucleobase and/or on the ribose sugar component have been established.[23–26] Among them, the arylethynyltriazole nucleosides stand out because of their extremely appealing antiviral and anticancer activities (**I–IV** in Fig. 1).[23,24,27–30] Importantly, novel mechanisms such as the inhibition of heat shock factor 1 (HSF1) and related heat shock proteins (HSPs) contribute to the anticancer activity of 3-arylethynyltriazole nucleoside[28] (**III** in Fig. 1), whereas the acyclic 5-arylethynyltriazole nucleoside (**IV** in Fig. 1) suppresses both HSF1 and androgen receptor expression to elicit anticancer activity in prostate cancer.[30] We are therefore interested in further developing 3-arylethynyltriazole acyclonucleosides **1** (Fig. 1), which are structural analogs of

[a] Chongqing Key Laboratory of Natural Product Synthesis and Drug Research, School of Pharmaceutical Sciences, Chongqing University, Chongqing, 401331, China. E-mail: yixia@cqu.edu.cn
[b] Shanghai Institute of Organic Chemistry, Chinese Academy of Sciences, Shanghai, 200032, China
[c] Aix-Marseille Université, CNRS, Centre Interdisciplinaire de Nanoscience de Marseille, UMR 7325, Equipe Labellisées Ligue Contre le Cancer, 13288 Marseille, France

† Electronic supplementary information (ESI) available: ^{1}H- and ^{13}C-NMR spectra of all new compounds, the synthesis of 1-(4-ethynylphenyl)-2,5,8,11,14,17,20-heptaoxahenicosane and iodotriazole **3**, full crystallographic data. CCDC 1441152, 1441261 and 1441262. For ESI and crystallographic data in CIF or other electronic format see DOI: 10.1039/c7nj01406f

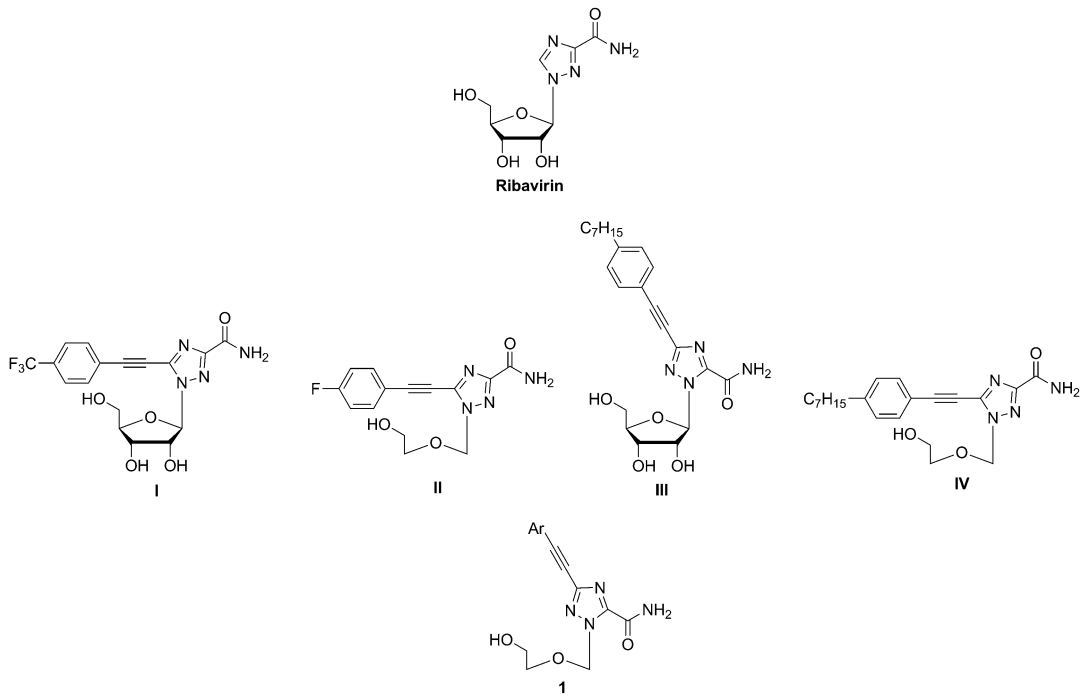

Fig. 1 Chemical structures of ribavirin, the identified arylethynyltriazole nucleosides with antiviral activity (**I–II**) and anticancer activity (**III–IV**), and the 3-arylethynyltriazole acyclonucleoside **1** proposed and synthesized in this work.

both **III** and **IV**; specifically, **1** is the acyclic analog of **III**, and at the same time, the 3-isomer of **IV**. With the nucleoside analog **1**, we aim to search for new leads as anticancer candidates and to enrich the structural diversity of the triazole nucleoside family for further analysis of structure–activity relationships. Herein, we report the preparation of 3-arylethynyltriazole acyclonucleoside **1** using the Sonogashira cross-coupling reaction, and the subsequent assessment of their antiproliferative effects on different cancer cells. Synthesis based on the Sonogashira reaction was achieved and significantly improved when using the 3-iodotriazole acyclonucleoside as the coupling substrate instead of the bromide derivative. Indeed, several synthesized compounds displayed antiproliferative activity against various cancer cells, outperforming ribavirin in the inhibition of drug-resistant pancreatic cancer cells. This finding highlights the potential of this family of triazole nucleosides as promising anticancer candidates.

Results and discussion

The Sonogashira cross-coupling reaction is a convenient strategy to introduce an arylalkynyl moiety into an aromatic system using an aryl halide and an aryl alkyne as the coupling substrates.[31,32] Based on our previous work on the synthesis of triazole nucleoside analogs,[23] we first attempted the Sonogashira cross-coupling reaction using the 3-bromotriazole acyclonucleoside **2a** as the aryl halide to couple with various alkynes in aqueous media under microwave (MW) irradiation[33,34] (Table 1, Method A). Using the previously established reaction conditions,[23] the Sonogashira reaction proceeded smoothly with most of the alkynes to deliver the corresponding products in good yields (Table 1, Method A). As shown in Table 1, there was no significant difference between the reactions using electron-donating phenylacetylenes (Table 1, entries 2–7, Method A) and those using electron-withdrawing substituents (Table 1, entries 8–12, Method A). Also, phenylacetylenes with fluorine substituted at the *ortho*-, *meta*- and *para*-positions afforded the corresponding products in very good yields (Table 1, entries 9–11, Method A). Nevertheless, the above-mentioned reaction conditions were not applicable to phenylacetylenes bearing the bromide (Table 1, entry 13, Method A) or the extremely electron-deficient nitro functionality (Table 1, entry 14, Method A) or the hexaethylene glycol methyl ether group (Table 1, entry 15, Method A): only trace or no corresponding product was obtained, with large amounts of **2a** remaining unreacted for **1n** and **1o**, whereas inseparable byproducts were formed for **1m**. The simultaneous and further continuous homo- and hetero-coupling with 4-bromophenylacetylene[35,36] as the substrate might be responsible for the low yield and inseparable byproducts when synthesizing **1m**. Formation of the undesirable Pd–O complex between the Pd-catalyst and the hexaethylene glycol methyl ether moiety might completely block the catalyst when preparing **1o**, whereas the strongly electron-deficient substituent of the nitro group may significantly decrease the nucleophilicity of the alkynes, hence impeding the Sonogashira reaction for generating the desired product.

To overcome the particular difficulty encountered in the Sonogashira reaction with these challenging alkyne substrates, we turned to the iodotriazole nucleoside **2b** as the halogen-bearing coupling substrate (Method B) because iodide compounds

Table 1 Synthesis of arylethynyltriazole acyclonucleoside **1** *via* the Sonogashira cross-coupling reaction using 3-bromotriazole acyclonucleoside **2a** (Method A) and 3-iodotriazole acyclonucleoside **2b** (Method B) as coupling substrates

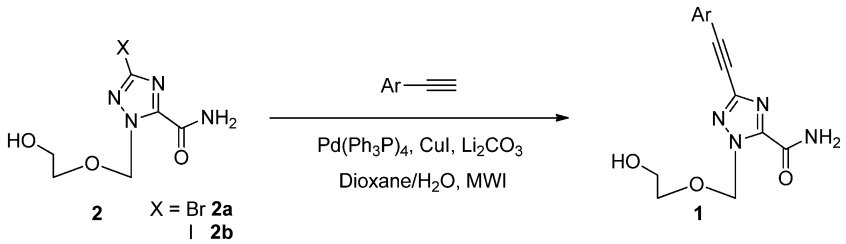

2 X = Br **2a**, I **2b** 1

Entry	Ar	Product	Method A[a] Yield (%)	Method B[b] Yield (%)
1		**1a**	87	88
2	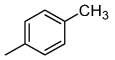	**1b**	83	92
3	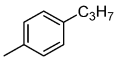	**1c**	88	91
4	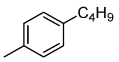	**1d**	79	97
5	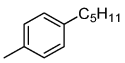	**1e**	79	97
6	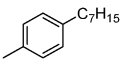	**1f**	84	89
7	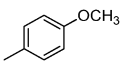	**1g**	79	97
8	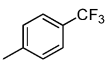	**1h**	82	92
9		**1i**	88	87
10		**1j**	95	96
11		**1k**	94	94
12	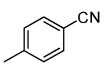	**1l**	70	81
13		**1m**	6	95
14	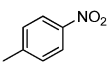	**1n**	5	90 (52)[a]
15	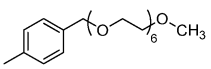	**1o**	NA	92

Reaction condition: [a] 100 °C, 1 hour. [b] 120 °C, 15 minutes. NA: not applicable.

are generally more reactive than bromide substrates in Pd-catalyzed cross-coupling reactions.[37,38] The iodotriazole acyclonucleoside **2b** was prepared *via* fusion of the iodotriazole **3** with the 2-(acetoxymethoxy)ethyl acetate **4** (Scheme 1), which generated a mixture of two isomeric products **5** and **5′**. We employed HMBC (Heteronuclear Multiple Bond Correlation) to discriminate between the two isomers **5** and **5′**. Compound **5** was assigned as the 3′-iodotriazole isomer based on the ^{1}H-NMR chemical shift of the methylene group (2*H*-C-1′) at 5.95 ppm and its HMBC cross peak with the carbon atom connected to the carboxylic ester group within the triazole heterocycle (δ 146.3, C-5) (Fig. 2A). Compound **5′** was designated as the 5′-iodotriazole isomer based on the ^{1}H-NMR chemical shift of the methylene group (2*H*-C-1′) at 5.64 ppm and its HMBC cross peak with the carbon connected to the iodide within the triazole ring (δ 101.7, C-5) (Fig. 2B). Subsequent ammonolysis of **5** and **5′** produced the corresponding iodotriazole acyclonucleosides **2b** and **2b′**, respectively, in good yields.

We then performed the Sonogashira reaction using **2b** under the same reaction conditions that we had elaborated with **2a**.

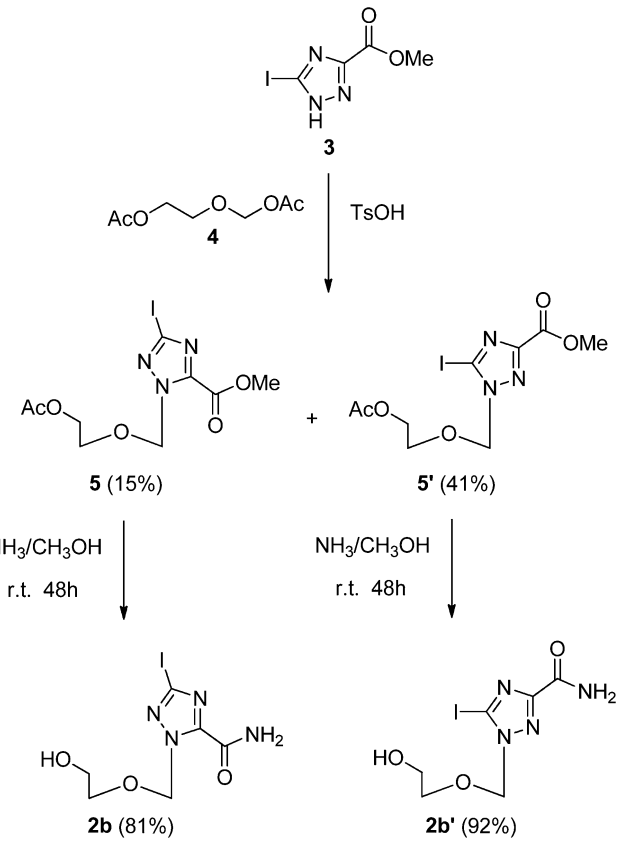

Scheme 1 Synthesis of the iodotriazole nucleosides **2b** and **2b′**.

Indeed, the reaction with 4-nitrophenylacetylene (Table 1, entry 14, Method B) afforded the desired product with a significantly increased yield of 52%. We further optimized the reaction conditions by varying the reaction temperature and time (data not shown). Excellent yields were achieved when **2b** was reacted with a wide range of alkynes under 15 minutes MW irradiation at 120 °C, regardless of the electron-donating or electron-withdrawing substituents on phenylacetylene (Table 1, Method B). Most importantly, the coupling reaction of **2b** with phenylacetylene carrying a bromide, or a nitro group or hexaethylene glycol methyl ether substitute also proceeded with excellent yields (Table 1, entries 13–15, Method B). This further confirms the superiority of the iodotriazole **2b** to the bromide **2a** for use in the Sonogashira reaction with challenging alkynes.

We further determined the structure of the 3-arylethynyl-triazole acyclonucleosides **1g** and **1h** using X-ray diffraction analysis (Fig. 3A and B). Remarkably, the triazole ring and the phenyl substituent approached almost complete coplanarity. This was strikingly different from the 5-arylethynyltriazole nucleoside **II** (Fig. 3C), where the phenyl ring adopted a different orientation (DO) from the 1,2,4-triazole unit because of steric hindrance from the neighboring sugar component. To gain further insight into the coplanarity, we studied and analyzed the different conformations of **1g** and **1h** generated using the program RandomSearch[39] of Sybyl 7.2.[40] In particular, we examined the conformation CO, in which the phenyl ring and the 1,2,4-triazole unit were almost coplanar, and the conformation DO, in which the phenyl ring

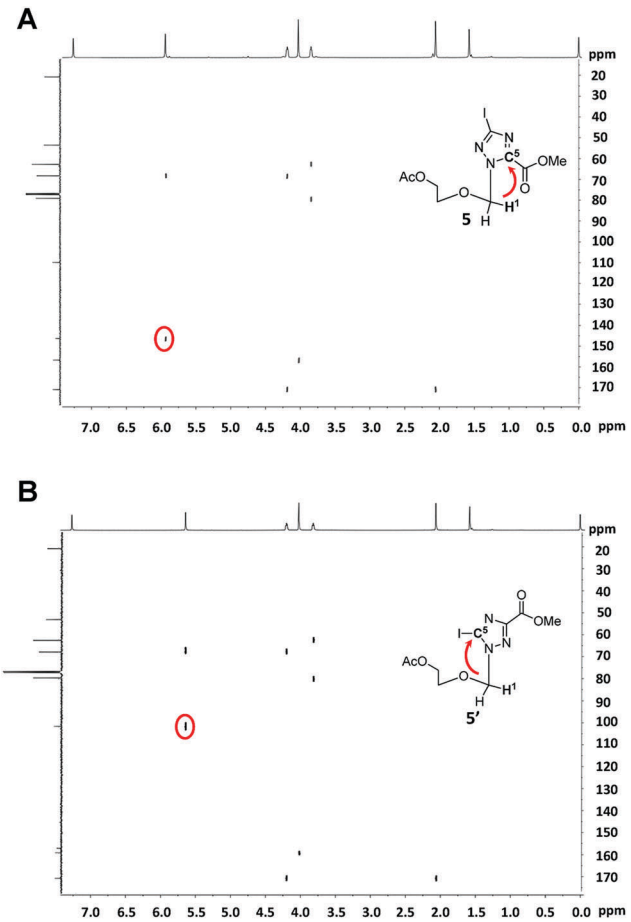

Fig. 2 ^{1}H-^{13}C HMBC spectrum of compounds **5** (A) and **5′** (B) in $CDCl_3$.

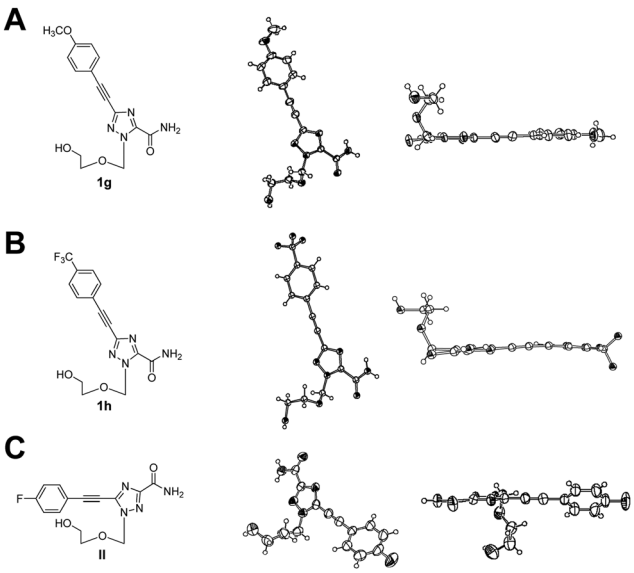

Fig. 3 Chemical and X-ray structures of **1g** (A), **1h** (B), and **II** (C). The triazole ring and the phenyl substituent approached almost complete co-planarity in **1g** (A) and **1h** (B), while in **II**, the phenyl ring adopted a different orientation from the 1,2,4-triazole unit (C).

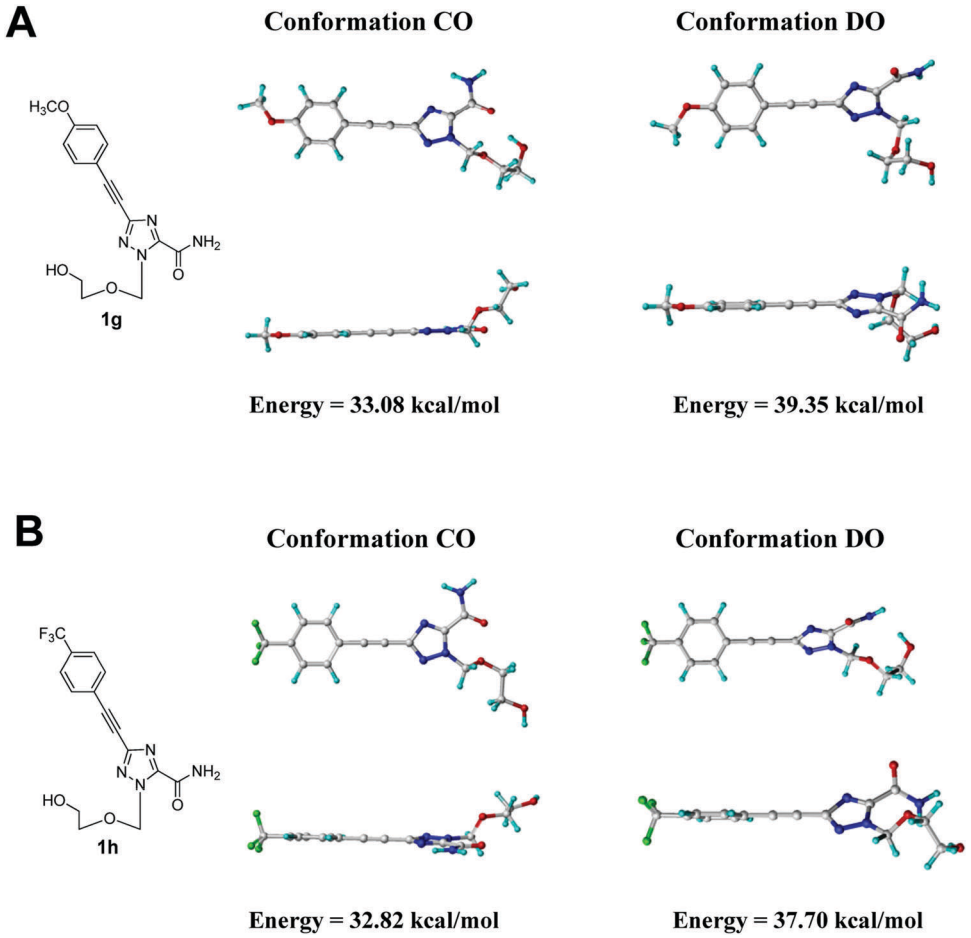

Fig. 4 The conformations CO and DO of (A) **1g** and (B) **1h** generated and analyzed using the program RandomSearch of Sybyl 7.2.

was in a different orientation from the 1,2,4-triazole unit. The CO conformations of **1g** and **1h** superimposed perfectly with the corresponding X-ray structures of **1g** and **1h**, respectively (Fig. 4). In addition, the total energy values for the CO conformations of **1g** and **1h** were 32.8 and 33.1 kcal mol^{-1}, respectively, which were much lower than those of the corresponding DO conformations (37.7 and 39.4 kcal mol^{-1}). These results further confirmed the higher stability of **1g** and **1h** with coplanar structures of the 3-arylethynyltriazole motifs, which might be considered as potential surrogates to mimic conjugated and enlarged nucleobases or aromatic systems.

With the aim of searching for novel anticancer candidates, we evaluated the anticancer activity of the synthesized nucleoside analog **1**. We assessed its antiproliferation activity on human pancreatic cancer BxPC-3 cells and prostate cancer PC-3 cells using the MTT assay for assessing cell metabolic activity. Several compounds were able to considerably inhibit the growth of both cell lines. Importantly, our compounds exhibited antiproliferation activity on BxPC-3 cells with potent IC_{50}, whereas the reference drug ribavirin did not show any activity within the same concentration range (Table 2). This result highlights the potential of this family of compounds in treating pancreatic cancer, one of the most deadly human cancers.[41,42] Among these active candidates, compounds **1e** and **1f** had a long hydrophobic alkyl chain attached to the phenyl group, while compound **1m** had the 4-bromophenyl substituent. Compared with **1e** and **1f**, the compounds **1c** and **1d** bearing shorter alkyl chains were inactive, suggesting the longer chain contributed importantly to the antiproliferation activity. Although **1e** was active against BxPC-3, it did not display any obvious inhibitory effect on pancreatic cancer MiaPaCa-2 cells in our previous study.[27] This is in agreement with a report that the nucleoside anticancer drug gemcitabine is also more efficient at inducing apoptosis in BxPC-3 cells than in MiaPaCa cells.[43] Also, the antiproliferation activity of **1f** in both cell lines was higher than its 5-analog **IV**, highlighting the

Table 2 Antiproliferation activity of 3-arylethynyltriazole nucleoside **1** on pancreatic cancer BxPC-3 cells and prostate cancer PC-3 cells

	IC_{50} (μM)			IC_{50} (μM)	
Compound	BxPC-3	PC-3	Compound	BxPC-3	PC-3
1a	>50	>50	**1i**	>50	>50
1b	>50	>50	**1j**	>50	>50
1c	>50	>50	**1k**	>50	>50
1d	>50	>50	**1l**	>50	>50
1e	22.5	23.3	**1m**	2.0	45.5
1f	8.33	17.5	**1n**	>50	>50
1g	>50	>50	**1o**	>50	>50
1h	39.3	>50			
Ribavirin	>50	>50	**IV**	17.5	32.2

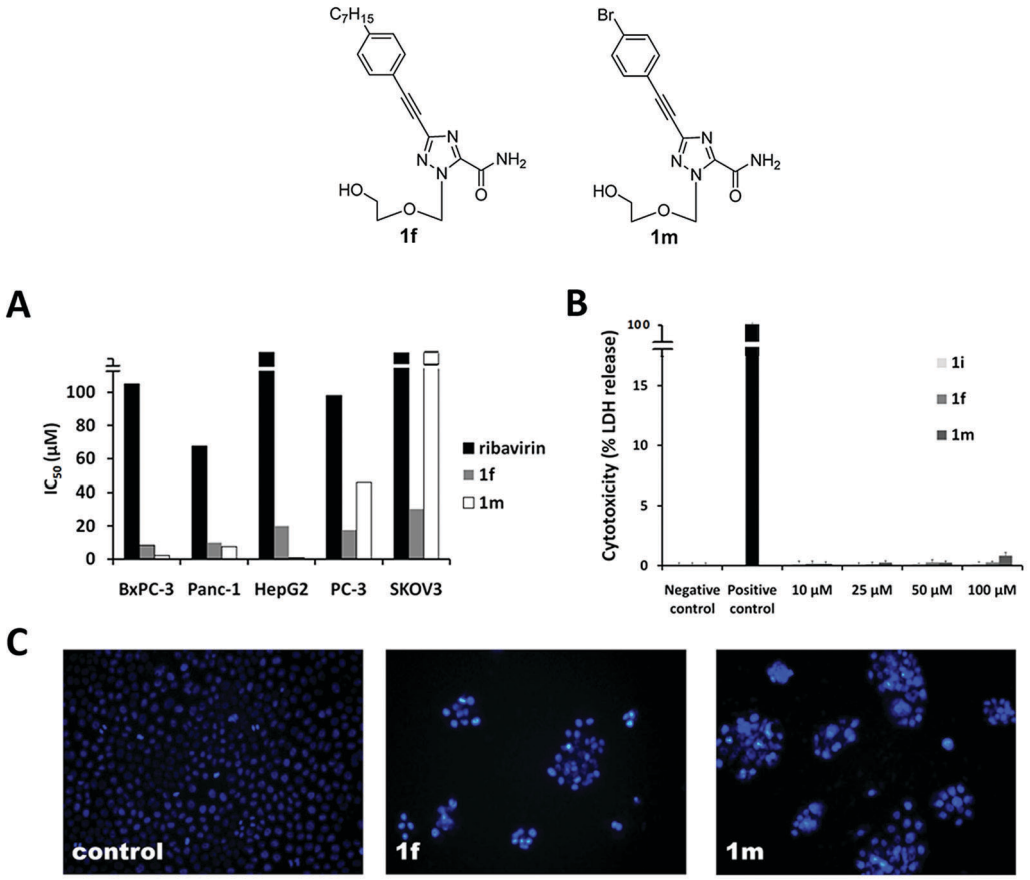

Fig. 5 (A) MTT assay to assess the ability of compounds **1f** and **1m** to inhibit the proliferation of human pancreatic cancer BxPC-3 and Panc-1 cells, human liver cancer HepG2 cells, human prostate cancer PC-3 cells, and human ovarian cancer SKOV3 cells; (B) LDH assay to assess the effects of **1i**, **1f**, and **1m** on PC-3 cells. The negative control shows the LDH activity released from untreated cells and the positive control shows the maximum LDH activity that could be released from the cells; (C) Hoechst 33342 staining to detect apoptosis in cultured BxPC-3 cells exposed to compounds **1f** and **1m**.

structural superiority of the 3′-arylethynyltriazole nucleosides (Table 2). We further evaluated the antiproliferation activity of **1f** and **1m** on other cancer cell lines such as pancreatic cancer Panc-1 cells, liver cancer HepG2 cells, and ovarian cancer SKOV3 cells. As shown in Fig. 5A, **1f** displayed similar inhibition activity on all the tested cell lines. Remarkably, **1m** was very active against the human pancreatic cancer cells BxPC-3 and Panc-1 and the liver cancer cell line HepG2, but was much less potent in suppressing prostate cancer and ovarian cancer cells. This suggests that **1m** has potential as an anticancer candidate for malignant gastrointestinal tumors.[44,45]

As **1f** possesses a long alkyl chain, we wanted to know whether it might cause cytotoxicity by disrupting the cell membrane and hence inducing membrane damage or leakage. As the release of lactate dehydrogenase (LDH) is a general indicator of membrane disintegration and destruction,[46] we therefore measured the LDH release from PC-3 cells. Our results showed that the active compounds **1f** and **1m**, like the inactive compound **1i**, did not cause significant LDH release even at high concentrations (Fig. 5B). This highlights that the antiproliferative activity demonstrated by **1f** and **1m** did not result from membrane-disrupting toxicity. Furthermore, it is known that apoptosis can be assessed by staining the cells with Hoechst 33342 dye, as apoptotic cells have condensed chromatin that stains more brightly than the chromatin in healthy cells.[47] As shown in Fig. 5C, the **1f**- and **1m**-treated BxPC-3 cells stained more brightly with Hoechst 33342 than the nontreated cells, suggesting that both triazole nucleoside compounds can efficiently induce apoptosis. These compounds hence constitute promising new hits in our continuing search for more efficacious drug candidates to combat cancers.

Conclusions

In summary, we have developed a series of 3-arylethynyltriazole acyclonucleosides **1** as novel nucleoside analogs in our quest for new anticancer lead compounds. Their synthesis was achieved using the Sonogashira coupling reaction with 3-iodotriazole nucleoside as the aryl halide coupling substrate, which delivered the corresponding products in excellent yields even with challenging alkyne substrates. Importantly, the 3-arylethynyltriazole motif is coplanar and may serve as a potential surrogate for large nucleobases or aromatic systems. Moreover, we assessed the antiproliferation activities of the synthesized nucleosides on various human cancer cells. Remarkably, several compounds

bearing either a long alkyl chain or a bromide group, showed potent anticancer activity against different cancer cell lines. This family of compounds hence constitutes promising leads for further analyses of structure–activity relationships with the aim of exploring more potent anticancer candidates and advancing our drug discovery program. We are working actively in this direction.

Experimental section

Instrumentation and chemicals

All the terminal alkynes and chemical reagents were purchased from Adamas-beta, Energy Chemical, Woka and TCI. Solvents were purchased from a local supplier and used without further purification beside THF. THF was distilled from sodium and benzophenone. All compounds were purified by performing flash chromatography on silica gel (200–300 mesh). ^{1}H NMR and ^{13}C NMR spectra were recorded on Agilent DD2 400-MR. ^{1}H-^{13}C HMBC spectra were recorded on Agilent DD2 600-MR. The chemical shifts were recorded in parts per million (ppm) with tetramethylsilane as the internal reference. The microwave-assisted reactions were performed on an Initiator EXP EU produced by Biotage. The ESI-MS was recorded on a Waters Acquity SQ Detecter mass spectrometer or Finigan LCQ mass spectrometer. The high resolution of ESI-MS was recorded on a Bruker SolariX 7.0T mass spectrometer or IonSpec 4.7 Tesla Fourier Transform mass spectrometer. All MS analysis samples were prepared as solutions in methanol.

Synthesis of 5 and 5′

A mixture of iodotriazole **3** (1.08 g, 4.29 mmol), 2-(acetoxymethoxy)ethyl acetate **4** (1.89 g, 10.72 mmol), and *p*-toluenesulfonic acid monohydrate (40.78 mg, 0.214 mmol) were heated at 140 °C for 5 min, then stirred at 140 °C under vacuum for 40 min. After being cooled to room temperature, the reaction mixture was introduced into a column (petroleum ether : ethyl acetate = 2 : 1) to afford **5** (241 mg, 15%) and **5′** (643 mg, 41%) as white solids.

3-Iodo-1-[(2-acetoxyethoxy)methyl]-1,2,4-triazole-5-carboxylate (5). White solid. ^{1}H NMR (400 MHz, $CDCl_3$) δ 5.95 (s, 2H), 4.19 (t, 2H, J = 4.8 Hz), 4.03 (s, 3H), 3.85 (t, 2H, J = 4.8 Hz), 2.06 (s, 3H). ^{13}C NMR (100 MHz, $CDCl_3$) δ 170.78, 156.71, 146.29, 109.89, 79.15, 68.26, 62.79, 53.59, 20.83. MS (ESI, m/z): 392.18 $[M + Na]^+$, 370.24 $[M + H]^+$.

5-Iodo-1-[(2-acetoxyethoxy)methyl]-1,2,4-triazole-3-carboxylate (5′). White solid. ^{1}H NMR (400 MHz, $CDCl_3$) δ 5.64 (s, 2H), 4.20 (t, 2H, J = 4.0 Hz), 4.02 (s, 3H), 3.82 (t, 2H, J = 4.0 Hz), 2.06 (s, 3H). ^{13}C NMR (100 MHz, $CDCl_3$) δ 170.76, 159.12, 157.03, 101.66, 79.71, 67.90, 62.60, 53.13, 20.86. MS (ESI, m/z): 392.25 $[M + Na]^+$, 370.24 $[M + H]^+$.

Synthesis of 2b and 2b′

5 (230 mg, 0.93 mmol) and **5′** (230 mg, 0.93 mmol) were dissolved separately in saturated NH_3 in MeOH (30 mL) at room temperature and stirred at room temperature for 48 h. The solvent was removed and residues were introduced into the column (dichloromethane : methanol = 20 : 1) to afford **2b** (158 mg, 81%) and **2b′** (179 mg, 92%) as white solids.

3-Iodo-1-[(2-hydroxyethoxy)methyl]-1,2,4-triazole-5-carboxamide (2b). White solid. ^{1}H NMR (400 MHz, DMSO-d_6) δ 8.39 (br, 1H), 8.08 (br, 1H), 5.87 (s, 2H), 4.68 (t, 1H, J = 4.8 Hz), 3.54 (t, 2H, J = 4.8 Hz), 3.43–3.46 (m, 2H). ^{13}C NMR (100 MHz, DMSO-d_6) δ 157.80, 149.68, 111.76, 78.77, 71.80, 60.22. MS (ESI, m/z): 335.25 $[M + Na]^+$, 313.20 $[M + H]^+$.

5-Iodo-1-[(2-hydroxyethoxy)methyl]-1,2,4-triazole-3-carboxamide (2b′). White solid. ^{1}H NMR (400 MHz, DMSO-d_6) δ 7.96 (br, 1H), 7.68 (br, 1H), 5.57 (s, 2H), 4.73 (t, 1H, J = 4.8 Hz), 3.54 (t, 2H, J = 4.8 Hz), 3.47–3.50 (m, 2H). ^{13}C NMR (100 MHz, DMSO-d_6) δ 160.02, 159.70, 106.41, 79.68, 71.58, 60.23. MS (ESI, m/z): 335.22 $[M + Na]^+$, 313.17 $[M + H]^+$.

General procedure for synthesis of 1

3-Halogen-1-[(2-hydroxyethoxy)methyl]-1,2,4-triazole-5-carboxamide (0.1 mmol), terminal alkyne (0.12 mmol), $Pd(Ph_3P)_4$ (5.8 mg, 0.005 mmol), CuI (1.0 mg, 0.005 mmol) and Li_2CO_3 (14.8 mg, 0.2 mmol) were suspended in dioxane/H_2O (3 : 1, 2 mL) at room temperature in a microwave reaction vessel, then N_2 was introduced into the vessel and it was sealed quickly. The mixture was reacted at 100 °C for 1 hour (Method A) or 120 °C for 15 minutes (Method B) under microwave (absorption level: high). After being cooled to room temperature, the solvent was removed and the residues were introduced into the column (dichloromethane : methanol = 40 : 1) to afford the product.

3-(2-Phenylethynyl)-1-[(2-hydroxyethoxy)methyl]-1,2,4-triazole-5-carboxamide (1a). White solid. ^{1}H NMR (400 MHz, DMSO-d_6) δ 8.47 (br, 1H), 8.11 (br, 1H), 7.64–7.65 (m, 2H), 7.47–7.52 (m, 3H), 5.94 (s, 2H), 4.68 (t, 1H, J = 5.6 Hz), 3.57–3.59 (m, 2H), 3.46–3.48 (m, 2H). ^{13}C NMR (100 MHz, DMSO-d_6) δ 158.29, 148.25, 145.54, 132.19, 130.45, 129.43, 120.76, 89.77, 80.36, 79.25, 71.87, 60.23. IR: 2234 cm^{-1} (–C≡C–). MS (ESI, m/z): 287.3 $[M + H]^+$, 309.3 $[M + Na]^+$, 595.4 $[2M + Na]^+$. HRMS: calcd for $C_{14}H_{14}N_4NaO^+$, $[M + Na]^+$, 309.0958; found, 309.0961.

3-[2-(*p*-Methyl)phenylethynyl]-1-[(2-hydroxyethoxy)methyl]-1,2,4-triazole-5-carboxamide (1b). White solid. ^{1}H NMR (400 MHz, DMSO-d_6) δ 8.45 (br, 1H), 8.10 (br, 1H), 7.52 (d, 2H, J = 7.6 Hz), 7.29 (d, 2H, J = 7.6 Hz), 5.93 (s, 2H), 4.68 (t, 1H, J = 5.6 Hz), 3.58 (t, 2H, J = 4.8 Hz), 3.46–3.49 (m, 2H), 2.36 (s, 3H). ^{13}C NMR (100 MHz, DMSO-d_6) δ 158.31, 148.19, 145.68, 140.46, 132.10, 130.03, 117.74, 90.05, 79.86, 79.22, 71.86, 60.23, 21.56. IR: 2225 cm^{-1} (–C≡C–). MS (ESI, m/z): 301.4 $[M + Na]^+$, 623.5 $[2M + Na]^+$, 299.3 $[M - H]^-$. HRMS: calcd for $C_{15}H_{16}N_4NaO_3^+$, $[M + Na]^+$, 323.1115; found, 323.1116.

3-[2-(*p*-Propyl)phenylethynyl]-1-[(2-hydroxyethoxy)methyl]-1,2,4-triazole-5-carboxamide (1c). White solid. ^{1}H NMR (400 MHz, DMSO-d_6) δ 8.47 (br, 1H), 8.11 (br, 1H), 7.54 (d, 2H, J = 8.4 Hz), 7.30 (d, 2H, J = 8.4 Hz), 5.93 (s, 2H), 4.69 (t, 1H, J = 5.6 Hz), 3.58 (t, 2H, J = 4.8 Hz), 3.44–3.48 (m, 2H), 2.60 (t, 2H, J = 7.6 Hz); 1.58–1.63 (m, 2H); 0.90 (t, 3H, J = 7.2 Hz). ^{13}C NMR (100 MHz, DMSO-d_6) δ 158.32, 148.18, 145.67, 145.02, 132.14, 129.45, 118.02, 90.06, 79.88, 79.22, 71.86, 60.23, 37.57, 24.24, 14.04. IR: 2225 cm^{-1} (–C≡C–). MS (ESI, m/z): 679.60 $[2M + Na]^+$, 351.47 $[M + Na]^+$,

327.38 $[M - H]^+$. HRMS: calcd for $C_{17}H_{20}N_4NaO_3^+$, $[M + Na]^+$, 351.1428; found, 351.1428.

3-[2-(*p*-Butyl)phenylethynyl]-1-[(2-hydroxyethoxy)methyl]-1,2,4-triazole-5-carboxamide (1d). White solid. ^{1}H NMR (400 MHz, DMSO-d_6) δ 8.46 (br, 1H), 8.11 (br, 1H), 7.53 (d, 2H, J = 7.6 Hz), 7.30 (d, 2H, J = 8.0 Hz), 5.93 (s, 2H), 4.68 (t, 1H, J = 5.6 Hz), 3.58 (t, 2H, J = 4.8 Hz), 3.45–3.48 (m, 2H), 2.63 (t, 2H, J = 7.6 Hz), 1.53–1.60 (m, 2H), 1.28–1.33 (m, 2H), 0.90 (t, 3H, J = 7.2 Hz). ^{13}C NMR (100 MHz, DMSO-d_6) δ 158.33, 148.14, 145.67, 145.26, 132.14, 129.41, 117.89, 90.11, 79.80, 79.21, 71.82, 60.20, 35.17, 33.21, 22.13, 14.18. IR: 2225 cm^{-1} (–C≡C–). MS (ESI, m/z): 707.61 $[2M + Na]^+$, 365.42 $[M + Na]^+$, 341.37 $[M - H]^+$. HRMS: calcd for $C_{18}H_{22}N_4NaO_3^+$, $[M + Na]^+$, 365.1584; found, 365.1584.

3-[2-(*p*-Pentyl)phenylethynyl]-1-[(2-hydroxyethoxy)methyl]-1,2,4-triazole-5-carboxamide (1e). White solid. ^{1}H NMR (400 MHz, DMSO-d_6) δ 8.49 (br, 1H), 8.12 (br, 1H), 7.54 (d, 2H, J = 8.0 Hz), 7.30 (d, 2H, J = 8.0 Hz), 5.93 (s, 2H), 4.70 (t, 1H, J = 5.6 Hz), 3.58 (t, 2H, J = 5.2 Hz), 3.44–3.48 (m, 2H), 2.62 (t, 2H, J = 7.6 Hz), 1.54–1.60 (m, 2H), 1.25–1.34 (m, 4H), 0.86 (t, 3H, J = 6.8 Hz). ^{13}C NMR (100 MHz, DMSO-d_6) δ 158.32, 148.18, 145.68, 145.25, 132.15, 129.39, 117.97, 90.06, 79.88, 79.22, 71.86, 60.23, 35.47, 31.27, 30.76, 22.38, 14.35. IR: 2224 cm^{-1} (–C≡C–). MS (ESI, m/z): 735.62 $[2M + Na]^+$, 379.49 $[M + Na]^+$, 355.37 $[M - H]^+$. HRMS: calcd for $C_{19}H_{25}N_4O_3^+$, $[M + H]^+$, 357.1921; found, 357.1911.

3-[2-(*p*-Heptyl)phenylethynyl]-1-[(2-hydroxyethoxy)methyl]-1,2,4-triazole-5-carboxamide (1f). White solid. ^{1}H NMR (400 MHz, DMSO-d_6) δ 8.46 (br, 1H), 8.11 (br, 1H), 7.53 (d, 2H, J = 8.0 Hz), 7.29 (d, 2H, J = 7.6 Hz), 5.94 (s, 2H), 4.68 (br, 1H), 3.59 (t, 2H, J = 4.8 Hz), 3.47–3.48 (m, 2H), 2.62 (t, 2H, J = 7.6 Hz), 1.57 (t, 2H, J = 6.4 Hz), 1.25–1.28 (m, 8H), 0.85 (t, 3H, J = 6.0 Hz). ^{13}C NMR (100 MHz, DMSO-d_6) δ 158.31, 148.19, 145.69, 145.22, 132.13, 129.36, 117.98, 90.04, 79.88, 79.22, 71.86, 60.24, 35.50, 31.65, 31.05, 29.01, 28.92, 22.50, 14.36. IR: 2225 cm^{-1} (–C≡C–). MS (ESI, m/z): 791.7 $[2M + Na]^+$. HRMS: calcd for $C_{21}H_{28}N_4NaO_3^+$, $[M + Na]^+$, 407.2054; found, 407.2057.

3-[2-(*p*-Methoxyl)phenylethynyl]-1-[(2-hydroxyethoxy)methyl]-1,2,4-triazole-5-carboxamide (1g). White solid. ^{1}H NMR (400 MHz, DMSO-d_6) δ 8.48 (br, 1H), 8.12 (br, 1H), 7.58 (d, 2H, J = 8.8 Hz), 7.03 (d, 2H, J = 8.8 Hz), 5.92 (s, 2H), 4.71 (t, 1H, J = 5.6 Hz), 3.81 (s, 3H), 3.57 (t, 2H, J = 5.2 Hz), 3.47 (t, 2H, J = 5.2 Hz). ^{13}C NMR (100 MHz, DMSO-d_6) δ 160.85, 158.34, 148.11, 145.83, 133.93, 115.09, 112.52, 90.15, 79.17, 71.83, 60.21, 55.83. IR: 2224 cm^{-1} (–C≡C–). MS (ESI, m/z): 339.31 $[M + Na]^+$, 317.32 $[M + H]^+$, 315.30 $[M - H]^+$. HRMS: calcd for $C_{15}H_{17}N_4O_4^+$, $[M + H]^+$, 317.1244; found, 317.1236.

3-[2-(*p*-Trifluoromethyl)phenylethynyl]-1-[(2-hydroxyethoxy)-methyl]-1,2,4-triazole-5-carboxamide (1h). White solid. ^{1}H NMR (400 MHz, DMSO-d_6) δ 8.48 (br, 1H), 8.14 (br, 1H), 7.83–7.88 (m, 3H), 5.95 (s, 2H), 4.69 (t, 1H, J = 5.6 Hz), 3.59 (t, 2H, J = 4.8 Hz), 3.46–3.49 (m, 2H). ^{13}C NMR (100 MHz, DMSO-d_6) δ 158.21, 148.38, 145.08, 133.04, 130.19 (q, J = 32 Hz), 126.24 (q, J = 3.6 Hz), 125.04, 124.20 (q, J = 270.9 Hz), 88.16, 82.54, 79.38, 79.11, 60.23. IR: 2025 cm^{-1} (–C≡C–). MS (ESI, m/z): 377.3 $[M + Na]^+$, 731.4 $[2M + Na]^+$, 353.3 $[M - H]^-$. HRMS: calcd for $C_{15}H_{13}F_3N_4NaO_3^+$, [M + Na]+, 377.0832; found, 377.0833.

3-[2-(*p*-Fluoro)phenylethynyl]-1-[(2-hydroxyethoxy)methyl]-1,2,4-triazole-5-carboxamide (1i). White solid. ^{1}H NMR (400 MHz, DMSO-d_6) δ 8.46 (br, 1H), 8.12 (br, 1H), 7.70–7.73 (m, 2H), 7.33 (t, 2H, J = 8.8Hz), 5.94 (s, 2H), 4.68 (t, 1H, J = 6.4 Hz), 3.58 (t, 2H, J = 4.8 Hz), 3.45–3.49 (m, 2H). ^{13}C NMR (100 MHz, DMSO-d_6) δ 163.17 (d, J = 248.0 Hz), 158.29, 148.26, 145.48, 134.75 (d, J = 8.8 Hz), 117.24 (d, J = 3.3 Hz), 116.78 (d, J = 22.2 Hz), 88.78, 80.17, 79.27, 71.88, 60.24. IR: 2230.56 cm^{-1} (–C≡C–). MS (ESI, m/z): 303 $[M - H]^-$. HRMS: calcd for $C_{14}H_{14}FN_4O_3^+$, $[M + H]^+$, 305.1044; found, 305.1041.

3-[2-(*o*-fluoro)phenylethynyl]-1-[(2-hydroxyethoxy)methyl]-1,2,4-triazole-5-carboxamide (1j). White solid. ^{1}H NMR (400 MHz, DMSO-d_6) δ 8.50 (br, 1H), 8.13 (br, 1H), 7.72 (td, 1H, J_1 = 7.6 Hz, J_2 = 1.6 Hz), 7.55–7.61 (m, 1H), 7.40 (t, 1H, J = 8.8 Hz), 7.32 (t, 1H, J = 7.6 Hz), 5.95 (s, 2H), 4.69 (t, 1H, J = 5.2 Hz), 3.59 (t, 2H, J = 4.8 Hz), 3.45–3.49 (m, 2H). ^{13}C NMR (100 MHz, DMSO-d_6) δ 162.30 (d, J = 249.5 Hz), 157.82, 147.93, 144.79, 133.80, 132.44 (d, J = 8.1 Hz), 125.12 (d, J = 3.3 Hz), 116.00 (d, J = 20.1 Hz), 108.81 (d, J = 15.2 Hz), 84.72, 82.77, 78.92, 71.47, 59.81. IR: 2236 cm^{-1} (–C≡C–). MS (ESI, m/z): 305.35 $[M + H]^+$. HRMS: calcd for $C_{14}H_{13}FN_4NaO_3^+$, $[M + Na]^+$, 327.0864; found, 327.0866.

3-[2-(*m*-Fluoro)phenylethynyl]-1-[(2-hydroxyethoxy)methyl]-1,2,4-triazole-5-carboxamide (1k). White solid. ^{1}H NMR (400 MHz, DMSO-d_6) δ 8.48 (br, 1H), 8.14 (br, 1H), 7.48–7.56 (m, 3H), 7.36–7.41 (m, 1H), 5.94 (s, 2H), 4.70 (t, 1H, J = 5.2 Hz), 3.58 (t, 2H, J = 5.2 Hz), 3.45–3.49 (m, 2H). ^{13}C NMR (100 MHz, DMSO-d_6) δ 162.28 (d, J = 243.8 Hz), 158.25, 148.32, 145.23, 131.66 (d, J = 8.7 Hz), 128.70 (d, J = 2.7 Hz), 122.65 (d, J = 9.5 Hz), 118.83 (d, J = 23.1 Hz), 117.88 (d, J = 20.9 Hz), 88.35, 81.12, 79.33, 71.90, 60.23. IR: 2236 cm^{-1} (–C≡C–). MS (ESI, m/z): 305.35 $[M + H]^+$. HRMS: calcd for $C_{14}H_{13}FN_4NaO_3^+$, $[M + Na]^+$, 327.0864; found, 327.0865.

3-[2-(*p*-Cyano)phenylethynyl]-1-[(2-hydroxyethoxy)methyl]-1,2,4-triazole-5-carboxamide (1l). White solid. ^{1}H NMR (400 MHz, DMSO-d_6) δ 8.52 (br, 1H), 8.17 (br, 1H), 7.97 (d, 2H, J = 8.4 Hz), 7.84 (d, 2H, J = 8.4 Hz), 5.95 (s, 2H), 4.72 (t, 1H, J = 5.6 Hz), 3.58 (t, 2H, J = 4.8 Hz), 3.44–3.48 (m, 2H). ^{13}C NMR (100 MHz, DMSO-d_6) δ 158.19, 148.41, 144.97, 133.25, 133.02, 125.51, 118.66, 112.68, 88.14, 83.74, 79.40, 71.91, 60.21. IR: 2235 cm^{-1} (–C≡C–), 2250 cm^{-1} (–C≡N). MS (ESI, m/z): 312.32 $[M + H]^+$, 334.31 $[M + Na]^+$. HRMS: calcd for $C_{15}H_{13}N_5NaO_3^+$, $[M + Na]^+$, 334.0911; found, 334.0911.

3-[2-(*p*-Bromo)phenylethynyl]-1-[(2-hydroxyethoxy)methyl]-1,2,4-triazole-5-carboxamide (1m). White solid. ^{1}H NMR (400 MHz, DMSO-d_6) δ 8.49 (br, 1H), 8.14 (br, 1H), 7.69 (d, 2H, J = 8.4 Hz), 7.59 (d, 2H, J = 8.4 Hz), 5.93 (s, 2H), 4.71 (t, 1H, J = 5.6 Hz), 3.57 (t, 2H, J = 4.8 Hz), 3.44–3.48 (m, 2H). ^{13}C NMR (100 MHz, DMSO-d_6) δ 158.25, 148.29, 145.34, 134.12, 132.53, 124.10, 119.95, 88.73, 81.42, 79.30, 71.88, 60.21; IR: 2228 cm^{-1} (–C≡C–). MS (ESI, m/z): 365.25 $[M + H]^+$, 387.24 $[M + Na]^+$. HRMS: calcd for $C_{14}H_{13}BrN_4NaO_3^+$, $[M + Na]^+$, 387.0063; found, 387.0062.

3-[2-(*p*-Nitryl)phenylethynyl]-1-[(2-hydroxyethoxy)methyl]-1,2,4-triazole-5-carboxamide (1n). Brown solid. ^{1}H NMR (400 MHz, DMSO-d_6) δ 8.50 (br, 1H), 8.30 (d, 2H, J = 8.4 Hz), 8.16 (br, 1H), 7.92 (d, 2H, J = 8.4 Hz), 5.95 (s, 2H), 4.70 (t, 1H, J = 4.8 Hz),

3.58 (t, 2H, J = 4.8 Hz), 3.46–3.48 (m, 2H). ^{13}C NMR (100 MHz, DMSO-d_6) δ 158.18, 148.47, 148.15, 144.90, 133.60, 127.34, 124.49, 87.84, 84.46, 79.44, 71.93, 60.22. IR: 2026 cm^{-1} (–C≡C–). MS (ESI, m/z): 354.37 $[M + Na]^+$, 332.31 $[M + H]^+$. HRMS: calcd for $C_{14}H_{13}N_5NaO_5^+$, $[M + Na]^+$, 354.0809; found, 354.0809.

3-[(4-(2,5,8,11,14,17,20-Heptaoxahenicosyl)phenylethynyl)]-1-[(2-hydroxyethoxy)methyl]-1,2,4-triazole-5-carboxamide (1o). Yellow solid. ^{1}H NMR (400 MHz, $CDCl_3$) δ 7.58 (d, 2H, J = 7.6 Hz), 7.36 (d, 2H, J = 7.6 Hz), 7.31 (br, 1H), 6.06 (s, 2H), 5.92 (br, 1H), 4.59 (s, 2H, phenyl), 3.79–3.80 (m, 2H), 3.74–3.75 (m, 2H), 3.65–3.68 (m, 22H), 3.54–3.56 (m, 2H), 3.38 (s, 3H). ^{13}C NMR (100 MHz, $CDCl_3$) δ 157.81, 146.63, 146.55, 140.20, 132.17, 127.55, 120.12, 90.52, 79.45, 78.90, 72.65, 71.88, 71.67, 70.62, 70.53, 70.44, 69.74, 61.42, 58.98, 29.67. IR: 2226 cm^{-1} (–C≡C–). MS (ESI, m/z): 595.60 $[M + H]^+$, 617.58 $[M + Na]^+$. HRMS: calcd for $C_{28}H_{42}N_4NaO_{10}^+$, $[M + Na]^+$, 617.2793; found, 617.2787.

X-ray structure determinations

All crystals were crystallized from the solvent of compounds in MeOH/CH_2Cl_2 (1 : 1). The X-ray diffraction measurements were carried out on a Rigaku Oxford Diffraction system equipped with Mo-kα radiation (λ = 0.71073 Å) using the ω-scan method. Ten sets of frames were measured to collect preliminary lattice parameters and orientation matrices. Some 6266 reflections were configured to obtain the unit cell dimensions. The structure was solved by a direct method using SHELXS(2008) and refined using full-matrix least-squares difference Fourier techniques by SHELXL-2014/7. All refinements were performed using the Olex2-1.2-alpha software package. All nonhydrogen atoms were refined with anisotropic displacement parameters and all H atoms were positioned geometrically and treated as riding on their parent C atoms with C–H distances of 0.93–0.97 Å, and with U_{iso}(H) = 1.2U_{eq}(C) for all C–H atoms.

Crystal data of 1a. $C_{14}H_{14}N_4O_3$, M_r = 286.29, orthorhombic, a = 11.4857(7) Å, b = 6.9956(4) Å, c = 33.950(3) Å, α = 90°, β = 90°, γ = 90°, V = 2727.8(3) Å^3, space group $Pbca$, Z = 8, D_{calc} = 1.394 g cm^{-3}, μ = 0.101 mm^{-1}, and F(000) = 1200.0. Crystal dimensions: 0.5 × 0.25 × 0.15 mm^3. Independent reflections: 2788 [R_{int} = 0.0226]. The final R_1 values were 0.0487 [$I \geq 2\sigma(I)$], wR_2 = 0.1368 [all data]. The goodness of fit on F^2 was 1.165. CCDC 1441462.†

Crystal data of 1g. $C_{15}H_{16}N_4O_4$, M_r = 316.32, monoclinic, a = 17.5680(9) Å, b = 9.9977(5) Å, c = 8.8328(5) Å, α = 90°, β = 104.264(6)°, γ = 90°, V = 1503.55(15) Å^3, space group $P2_1/c$, Z = 4, D_{calc} = 1.397 g cm^{-3}, μ = 0.104 mm^{-1}, and F(000) = 664.0. Crystal dimensions: 0.3 × 0.25 × 0.08 mm^3. Independent reflections: 3071 [R_{int} = 0.0229]. The final R_1 values were 0.0518 [$I \geq 2\sigma(I)$], wR_2 = 0.1418 [all data]. The goodness of fit on F^2 was 1.051. CCDC 1441262.†

Crystal data of 1h. $C_{15}H_{13}F_3N_4O_3$, M_r = 354.29, monoclinic, a = 35.076(3) Å, b = 10.0258(6) Å, c = 8.8087(5) Å, α = 90°, β = 94.027(6)°, γ = 90°, V = 3090.1(4) Å^3, space group $C2/c$, Z = 8, D_{calc} = 1.523 g cm^{-3}, μ = 0.132 mm^{-1}, and F(000) = 1456.0. Crystal dimensions: 0.3 × 0.3 × 0.2 mm^3. Independent reflections: 3552 [R_{int} = 0.0144]. The final R_1 values were 0.0577 [$I \geq 2\sigma(I)$], wR_2 = 0.1627 [all data]. The goodness of fit on F^2 was 1.083. CCDC 1441152.†

Conformation study

The different conformations of **1g** and **1h** were generated using RandomSearch[39] of Sybyl 7.2.[40] And the energies of conformation CO and DO were calculated using the same software.

Cell culture and reagents

Human prostate cancer PC-3, liver cancer HepG2 and ovarian cancer SKOV3 cells were purchased from the Cell Resource Centre, IBMS, CAMS/PUMC. Human pancreatic cancer Panc-1 and BxPC-3 cells were gifts from Prof. Huaizhi Wang (Institute of Hepatopancreatobiliary Surgery, Southwest Hospital, Chongqing). Panc-1 and BxPC-3 cells were grown at Roswell Park Memorial Institute 1640 (RPMI 1640) (GIBCO) supplemented with 10% FBS. HepG2 cells were grown in Dulbecco's modified Eagle's medium (DMEM) (HyClone) supplemented with 10% fetal bovine serum (FBS). PC-3 cells were grown in Ham's F12 (Kaighn's modification) (GIBCO) supplemented with 10% FBS. SKOV3 cells were grown in McCoy's 5A (GIBCO) supplemented with 10% FBS. Ribavirin and (3-(4,5-dimethylthiazol-2-yl)-2,5diphenyltetrazolium bromide, MTT) were purchased from Adamas. An LDH Cytotoxicity Assay Kit was purchased from Beyotime.

Cell growth inhibition assay

PC-3, HepG2, and SKOV3 cells were seeded into a 96-well plate at 10 000 cells per well, while BxPC-3 and Panc-1 cells were seeded at 5000 cells per well, and allowed to adhere overnight. Then, the culture medium was removed and replaced with fresh media alone as a control or containing various concentrations of the compounds. After 72 h of treatment, the number of viable cells remaining was determined using a (3-(4,5-dimethylthiazol-2-yl)-2,5diphenyltetrazolium bromide, MTT) colorimetric assay. All experiments were done in triplicate and repeated three independent times.

Lactate dehydrogenase (LDH) assay

The LDH assay was measured using a commercial LDH kit (Cytotoxicity Assay Kit, Beyotime). PC-3 cells were seeded 15 000 cells per well in 96-well plates. Some 24 hours later, the culture medium was removed and replaced with fresh media alone or containing the test compound. After 6 h treatment, the plates were centrifuged for 5 minutes in a multiwell plate centrifuge (400 g), and 120 μL supernatant of each well was transferred to a new 96-well plate. The LDH reaction mixture was freshly prepared according to the manufacturer's protocol and 60 μL of this mixture was added to each well of the plates containing blank, control, or cells in culture. The plate was incubated at 25 °C for 30 min. The control was performed with a release agent and blank medium, and set as 100% and 0% LDH release, respectively. The relative LDH release was defined by the ratio of LDH released over total LDH in the cells. All samples were performed in triplicate.

Hoechst 33342 staining assay

The Hoechst 33342 staining assay was measured using a commercial Hoechst 33342 staining solution (Beyotime). BxPC-3 cells

were seeded into a 96-well plate at 5000 cells per well and allowed to adhere overnight. Then, the culture medium was removed and replaced with fresh media (200 μL) alone as control or containing various compounds. After 48 h treatment, 10% glutaraldehyde solution (20 μL) was added to the wells for 10 min at 25 °C to fix the cells. Then, the solution was removed and the cells were washed three times with PBS. The Hoechst 33342 staining solution was added as 100 μL per well and incubated at 37 °C for 10 min. After the wash step, the cells were observed by fluorescence microscopy (Olympus IX51) to evaluate the apoptosis induced by the compounds.

Acknowledgements

Financial support from the National Natural Science Foundation of China (81502920), the Startup Funding for ''Hundred Young-Talent Program'' Professorship provided by Chongqing University (0236011104412), the Chongqing Natural Science Foundation (cstc2015jcyjA10093), the Fundamental Research Funds for the Central Universities (106112017CDJQJ468823 and 106112017CDJQJ158835), the Instrumental Analysis Foundation of Chongqing University (201606150012, 201512150027) and the La Ligue contre Le Cancer. We thank Mr Xiangnan Gong for the X-ray structure analysis.

Notes and references

1 C. Simons, *Nucleoside mimetics: their chemistry and biological properties.*, Gordon and Breach Science Publishers, Amsterdam, 2001.
2 B. Ewald, D. Sampath and W. Plunkett, *Oncogene*, 2008, **27**, 6522–6537.
3 P. J. Pockros, *Clin. Liver Dis.*, 2013, **17**, 105–110.
4 L. P. Jordheim, D. Durantel, F. Zoulim and C. Dumontet, *Nat. Rev. Drug Discovery*, 2013, **12**, 447–464.
5 J. Shelton, X. Lu, J. A. Hollenbaugh, J. H. Cho, F. Amblard and R. F. Schinazi, *Chem. Rev.*, 2016, **116**, 14379–14455.
6 V. Vivet-Boudou, J. C. Paillart, A. Burger and R. Marquet, *Nucleosides, Nucleotides Nucleic Acids*, 2007, **26**, 743–746.
7 R. E. Avanzo, C. Anesini, M. L. Fascio, M. I. Errea and N. B. D'Accorso, *Eur. J. Med. Chem.*, 2012, **47**, 104–110.
8 M. Hamada, V. Roy, T. R. McBrayer, T. Whitaker, C. Urbina-Blanco, S. P. Nolan, J. Balzarini, R. Snoeck, G. Andrei, R. F. Schinazi and L. A. Agrofoglio, *Eur. J. Med. Chem.*, 2013, **67**, 398–408.
9 A. A. A. Smith, K. Zuwala, M. B. L. Kryger, B. M. Wohl, C. Guerrero-Sanchez, M. Tolstrup, A. Postma and A. N. Zelikin, *Chem. Sci.*, 2015, **6**, 264–269.
10 C. H. Zhou and Y. Wang, *Curr. Med. Chem.*, 2012, **19**, 239–280.
11 X. M. Peng, G. X. Cai and C. H. Zhou, *Curr. Top. Med. Chem.*, 2013, **13**, 1963–2010.
12 S. Raic-Malic and A. Mescic, *Curr. Med. Chem.*, 2015, **22**, 1462–1499.
13 J. Zeidler, D. Baraniak and T. Ostrowski, *Eur. J. Med. Chem.*, 2015, **97**, 409–418.
14 S. Crotty, D. Maag, J. J. Arnold, W. Zhong, J. Y. Lau, Z. Hong, R. Andino and C. E. Cameron, *Nat. Med.*, 2000, **6**, 1375–1379.
15 J. D. Graci and C. E. Cameron, *Virology*, 2002, **298**, 175–180.
16 J. J. Feld, I. M. Jacobson, M. S. Sulkowski, F. Poordad, F. Tatsch and J. M. Pawlotsky, *Liver Int.*, 2017, **37**, 5–18.
17 C. Koh and T. J. Liang, *Antiviral Res.*, 2014, **104**, 34–39.
18 E. Thomas, M. G. Ghany and T. J. Liang, *Antiviral Chem. Chemother.*, 2012, **23**, 1–12.
19 K. L. Borden and B. Culjkovic-Kraljacic, *Leuk. Lymphoma*, 2010, **51**, 1805–1815.
20 B. C. Kraljacic, M. Arguello, A. Amri, G. Cormack and K. Borden, *Leukemia*, 2011, **25**, 1197–1200.
21 C. M. Galmarini, J. R. Mackey and C. Dumontet, *Leukemia*, 2001, **15**, 875–890.
22 Y. Xia, F. Qu and L. Peng, *Mini-Rev. Med. Chem.*, 2010, **10**, 806–821.
23 R. Zhu, M. Wang, Y. Xia, F. Qu, J. Neyts and L. Peng, *Bioorg. Med. Chem. Lett.*, 2008, **18**, 3321–3327.
24 J. Wan, Y. Xia, Y. Liu, M. Wang, P. Rocchi, J. Yao, F. Qu, J. Neyts, J. L. Iovanna and L. Peng, *J. Med. Chem.*, 2009, **52**, 1144–1155.
25 Y. Xia, M. Wang, O. Demaria, J. Tang, P. Rocchi, F. Qu, J. L. Iovanna, L. Alexopoulou and L. Peng, *J. Med. Chem.*, 2012, **55**, 5642–5646.
26 J. Tang, M. Cong, Y. Xia, G. Quelever, Y. Fan, F. Qu and L. Peng, *Org. Biomol. Chem.*, 2015, **13**, 110–114.
27 Y. Xia, Y. Liu, J. Wan, M. Wang, P. Rocchi, F. Qu, J. L. Iovanna and L. Peng, *J. Med. Chem.*, 2009, **52**, 6083–6096.
28 Y. Xia, Y. Liu, P. Rocchi, M. Wang, Y. Fan, F. Qu, J. L. Iovanna and L. Peng, *Cancer Lett.*, 2012, **318**, 145–153.
29 M. Wang, Y. Xia, Y. Fan, P. Rocchi, F. Qu, J. L. Iovanna and L. Peng, *Bioorg. Med. Chem. Lett.*, 2010, **20**, 5979–5983.
30 Y. Xia, M. Wang, E. Beraldi, M. Cong, A. Zoubeidi, M. Gleave and L. Peng, *Anti-Cancer Agents Med. Chem.*, 2015, **15**, 1333–1340.
31 R. Chinchilla and C. Najera, *Chem. Soc. Rev.*, 2011, **40**, 5084–5121.
32 C. C. Johansson Seechurn, M. O. Kitching, T. J. Colacot and V. Snieckus, *Angew. Chem., Int. Ed.*, 2012, **51**, 5062–5085.
33 V. Roy, U. Pradère and L. A. Agrofoglio, *Future Med. Chem.*, 2010, **2**, 177–192.
34 C. O. Kappe and D. Dallinger, *Nat. Rev. Drug Discovery*, 2006, **5**, 51–63.
35 J. P. Wan, S. Cao and Y. Jing, *Appl. Organomet. Chem.*, 2014, **28**, 631–634.
36 L. Su, J. Dong, L. Liu, M. Sun, R. Qiu, Y. Zhou and S. F. Yin, *J. Am. Chem. Soc.*, 2016, **138**, 12348–12351.
37 E. Negishi and L. Anastasia, *Chem. Rev.*, 2003, **103**, 1979–2017.
38 N. Kambe, T. Iwasaki and J. Terao, *Chem. Soc. Rev.*, 2011, **40**, 4937–4947.
39 M. Saunders, *J. Am. Chem. Soc.*, 1987, **109**, 3150–3152.
40 http://www.tripos.com.
41 I. Garrido-Laguna and M. Hidalgo, *Nat. Rev. Clin. Oncol.*, 2015, **12**, 319–334.

42 J. Kleeff, M. Korc, M. Apte, C. La Vecchia, C. D. Johnson, A. V. Biankin, R. E. Neale, M. Tempero, D. A. Tuveson, R. H. Hruban and J. P. Neoptolemos, *Nat. Rev. Dis. Primers*, 2016, **2**, 16022.

43 Y. Tomimaru, H. Eguchi, H. Wada, A. Tomokuni, S. Kobayashi, S. Marubashi, Y. Takeda, M. Tanemura, K. Umeshita, M. Mori, Y. Doki and H. Nagano, *Int. J. Oncol.*, 2011, **38**, 1237–1243.

44 E. Papadopoulou, V. Metaxa-Mariatou, G. Tsaousis, N. Tsoulos, A. Tsirigoti, C. Efstathiadou, A. Apessos, K. Agiannitopoulos, G. Pepe, E. Bourkoula and G. Nasioulas, *World J. Gastrointest. Oncol.*, 2016, **8**, 772–785.

45 M. Cives and J. Strosberg, *Curr. Treat. Options Oncol.*, 2017, **18**, 14.

46 V. Jurisic, S. Radenkovic and G. Konjevic, in *Advances in Cancer Biomarkers: From biochemistry to clinic for a critical revision*, ed. R. Scatena, Springer, Netherlands, Dordrecht, 2015, vol. 867, pp. 115–124.

47 B. Zhivotosky and S. Orrenius, *Current Protocols in Cell Biology*, John Wiley & Sons, Inc., 2001.